

Contribution from the Anorganisch-chemisches Institut der Universität Zürich, CH-8057 Zürich, Switzerland, and Laboratorium für Neutronenstreuung, Eidgenössische Technische Hochschule Zürich, CH-5303 Würenlingen, Switzerland

Magnetic Properties of Nickelocene. A Reinvestigation Using Inelastic Neutron Scattering and Magnetic Susceptibility

Philippe Baltzer,*^{1a} Albert Furrer,^{1b} Jürg Hulliger,^{1a} and Anton Stebler^{1a}

Received February 24, 1986

The magnetic properties of nickelocene, undiluted and doped into ruthenocene and ferrocene, have been determined by susceptibility measurements on powder samples and crystallites oriented in high magnetic fields, respectively, between 4.4 and about 200 K. The results reveal that there is a predominantly ferromagnetic coupling of a nickelocene molecule to its nearest neighbors in an undiluted sample, whereas the interaction with triplet-state molecules at greater distances in diluted samples seems to be anti-ferromagnetic. By introduction of two molecular fields, describing the intermolecular interactions and an intramolecular zero-field splitting, the magnetic susceptibility of nickelocene, undiluted and doped into isostructural diamagnetic hosts, can be interpreted by the same spin-Hamiltonian parameters: $D_0 = 33.6 \pm 0.3 \text{ cm}^{-1}$, $\Gamma_p = 0.63 \text{ cm}^{-1}$, and $\Gamma_s = 0.89 \text{ cm}^{-1}$. Furthermore the singlet-triplet separation in polycrystalline $\text{Ni}(\text{C}_5\text{D}_5)_2$ has been determined by inelastic neutron scattering (INS) spectroscopy. The observed magnetic transition at $31.6 \pm 1.0 \text{ cm}^{-1}$ in the INS spectra does not correspond directly to the zero-field splitting of the isolated molecule, D_0 , but shows some influence of the intermolecular coupling and the deuteriated ligands.

I. Introduction

Among the metallocenes (bis(cyclopentadienyl) transition-metal compounds), nickelocene is one of the most stable compounds; therefore, it has been synthesized and characterized in the beginning of organometallic chemistry.²⁻⁵ Its magnetic moment was reported to be $\mu = 2.86 \pm 0.1 \mu_B$, which is almost the spin-only value of a spin triplet and can be rationalized by the occupation of the 3d orbitals of Ni(II) in a ligand field of symmetry D_{5d} as shown in Figure 1.

A deviation of magnetic susceptibility from normal Curie-Weiss behavior below 70 K was reported by Leipfinger without further discussion.⁵ Nussbaum and Voitländer failed in measuring an EPR signal of nickelocene.⁶ They showed, with crystal field calculations, that a substantial axial zero-field splitting (about $+35 \text{ cm}^{-1}$) must be responsible for the lack of an EPR signal.

Prins et al.⁷ interpreted their susceptibility measurements on powder samples between 300 and 6.5 K in terms of an axial g tensor ($g_{\perp} = 2.06 \pm 0.1$, $g_{\parallel} = 2.0023$) and an axial zero-field splitting of $D = 25.6 \pm 3.0 \text{ cm}^{-1}$. A different value for D was found by Russian authors with measurements on single crystals ($D = 29.9 \text{ cm}^{-1}$).⁸ This value was confirmed by Oswald ($D = 29.0 \pm 1.6 \text{ cm}^{-1}$).⁹

Taking into account the lack of an EPR signal, Ammeter and Swalen used nickelocene as a quasi-diamagnetic host for EPR investigations of the doublet system cobaltocene,¹⁰ but the g values of cobaltocene in nickelocene were shifted compared to those values in a diamagnetic host (i.e. ferrocene). They suggested that this is due to an intermolecular coupling between the triplet system of the host and the doublet system investigated.

The susceptibility results of Zvarykina et al.⁸ confirm intermolecular coupling in nickelocene. The small deviation from the theoretical value of 2.0 (about 2.08) for the ratio of the constant susceptibility at low temperature perpendicular to and in the *ab* plane of the crystal (see Figure 2a for crystal structure) can be

interpreted with an intermolecular coupling, as we will show.

Recent EPR investigations on doublet systems doped into nickelocene showed exchange couplings on the order of some wavenumbers in the lattice of nickelocene.¹¹

To elucidate the magnetic behavior of nickelocene, we have reinvestigated the magnetic susceptibility of this compound, both undiluted and doped into diamagnetic hosts. In addition, we used inelastic neutron scattering (INS) to measure the energy difference ΔE between ground-state and excited-state levels within the triplet state directly. Compared to the results reported earlier,⁷⁻⁹ all spin-Hamiltonian parameters are modified and two molecular field constants are introduced for the undiluted nickelocene.

2. Experimental Section

2.1. Sample Preparation. We are indebted to Dr. A. Salzer from the University of Zürich, Switzerland, for providing samples of $\text{Ni}(\text{C}_5\text{D}_5)_2$ for INS investigations. The degree of deuteration of the final product was better than 90%.

The compounds for susceptibility measurements were prepared by following standard syntheses (ferrocene,¹² ruthenocene,¹³ nickelocene¹⁴). Nickelocene was purified by repeated vacuum sublimation at about 50 °C. Ruthenocene and ferrocene were doped with nickelocene by cosublimation of the diamagnetic host and the paramagnetic guest in an apparatus with two Knudsen cells having 0.4- and 0.1-mm diameters of the outlet, respectively.¹¹ The concentration of the guest molecule could be changed by variation of the temperature of sublimation for both, host and guest.

2.2. Magnetic Susceptibility. The magnetic susceptibility was measured on a Faraday balance similar to that described by Gardner and Smith¹⁵ supplied by Oxford Instruments Ltd. The measurements were performed at a main field between 10 and 19 kG and gradient fields of 300, 500 and 700 G/cm. The field was calibrated by using the common standard $\text{HgCo}(\text{NCS})_4$ ¹⁶ at room temperature, and the calibration was checked with tetramethylethylenediammonium tetrachlorocuprate(II)¹⁷ between 4 and 300 K. The powders for isotropic susceptibility measurements were pressed and sealed into a cylinder of aluminum foil as described earlier.¹⁹ To avoid time-consuming measurements on a crystallographically oriented single crystal, we also measured the susceptibility on loosely packed powder samples that were oriented in high magnetic fields, giving the value of the magnetic susceptibility along a

- (1) (a) Universität Zürich. (b) Laboratorium für Neutronenstreuung Würenlingen.
- (2) Fischer, E. O.; Jira, R. Z. *Naturforsch. B: Anorg. Chem., Org. Chem., Biochem., Biophys., Biol.* **1953**, *8B*, 217.
- (3) Engelmann, F. Z. *Naturforsch., B: Anorg. Chem., Org. Chem., Biochem., Biophys., Biol.* **1953**, *8B*, 775.
- (4) Wilkinson, G.; Pauson, R. L.; Cotton, F. A. J. *Am. Chem. Soc.* **1954**, *76*, 1970.
- (5) Leipfinger, H. Z. *Naturforsch., B: Anorg. Chem., Org. Chem., Biochem., Biophys., Biol.* **1958**, *13B*, 53.
- (6) Nussbaum, M.; Voitländer, J. Z. *Naturforsch., A: Astrophys., Phys., Phys. Chem.* **1965**, *20A*, 1417.
- (7) Prins, R.; van Voorst, J. D. W.; Schinkel, C. J. *Chem. Phys. Lett.* **1967**, *1*, 54.
- (8) Zvarykina, A. V.; Karimov, Yu. S.; Leonova, E. V.; Lyubovskii, R. B. *Sov. Phys.—Solid State (Engl. Transl.)* **1970**, *12*, 385.
- (9) Oswald, N. Ph.D. Thesis No. 5922, ETH Zürich, 1977.
- (10) Ammeter, J. H.; Swalen, J. D. *J. Chem. Phys.* **1972**, *57*, 678.

- (11) Hulliger, J. Ph.D. Thesis, University of Zürich, 1984.
- (12) Brauer, G. *Handbuch der präparativen anorganischen Chemie*, 3rd ed.; Enke: Stuttgart, West Germany, 1981; Vol. III.
- (13) Petrici, P.; Vetulli, G.; Paci, M.; Parri, L. *J. Chem. Soc., Dalton Trans.* **1980**, 1961.
- (14) Cordes, J. F. *Chem. Ber.* **1962**, *95*, 3084.
- (15) Gardner, W. E.; Smith, T. F. *Prog. Vac. Microbalance Tech.* **1972**, *9*, 155.
- (16) Bünzli, J. C. *Inorg. Chim. Lett.* **1979**, *36*, 413.
- (17) Brown, D. B.; Crawford, V. H.; Hall, J. W.; Hatfield, W. E. *J. Phys. Chem.* **1977**, *81*, 1303.
- (18) Baltzer, P.; Hulliger, J. *Inorg. Chem.* **1984**, *23*, 4772.
- (19) Hulliger, J.; Zoller, L.; Ammeter, J. H. *J. Magn. Reson.* **1982**, *48*, 512.

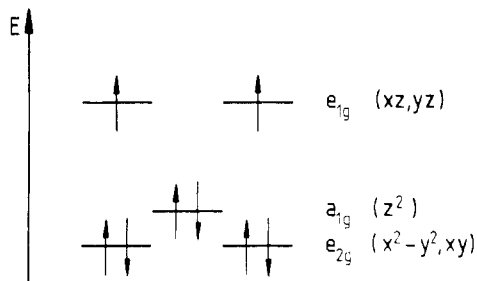


Figure 1. Energy splitting of 3d orbitals in a ligand field of symmetry D_{5d} and orbital occupation for nickelocene in the ${}^3A_{2g}$ ground state.

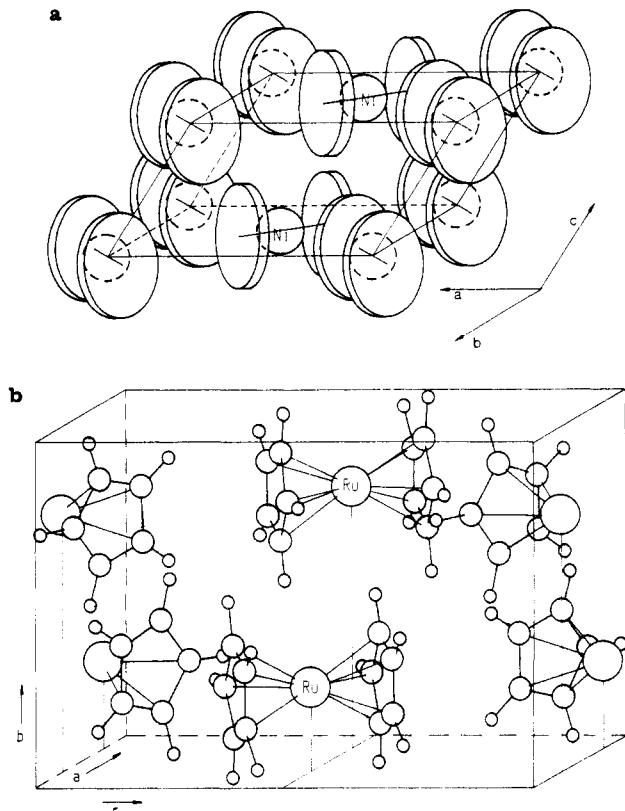


Figure 2. (a) Schematic view of the structure of nickelocene (after ref 8). (b) Crystal structure of ruthenocene (after ref 25).

principal molecular axis. The orientation of loosely packed powders was performed with a field of 64 kG shaking the samples at 4 K. EPR experiments on similar samples showed that such crystallites orient almost perfectly at even lower fields.¹⁸ Although shaking the samples was more difficult for the susceptibility experiments, we assumed that the same good degree of orientation was obtained due to the large field.^{18,19} The crystal structure of nickelocene (Figure 2a) and eq 4 and 6 show that all crystallites in a powder will orient with the ab plane perpendicular to the applied field under these conditions. In a similar manner, a crystal of ruthenocene (see Figure 2b) doped with nickelocene will align along the b axis.

Since both metallocenes have the same molecular structure (mean metal to carbon distance at 101 K: 2.186 Å (ruthenocene)²⁰ and 2.185 Å (nickelocene)²¹), ruthenocene can easily be replaced by nickelocene without disturbing the crystal structure. In fact, the lines of the X-ray powder pattern showed only a slight change when nickelocene was doped into ruthenocene.¹¹ In addition to the usual isotropic susceptibility value, the method of orientation of loosely packed powders allowed us to measure χ_{\parallel} of the undiluted nickelocene and χ_{\perp} of the molecule doped into ruthenocene.

2.3. Inelastic Neutron Scattering. Due to the large incoherent scattering contribution of ${}^1\text{H}$, undeuterated samples are not well suited for

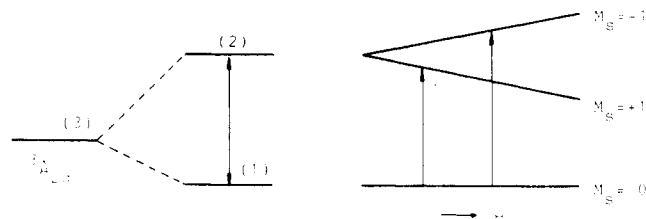


Figure 3. Energy level splitting of the nickelocene ground state in a magnetic field parallel to the axial zero field.

the study of magnetic excitations by thermal neutrons. Experiments were therefore performed on polycrystalline $\text{Ni}(\text{C}_5\text{D}_5)_2$, sealed into an aluminum cylinder of 8-mm diameter and 5-cm length.

All the neutron inelastic scattering experiments were performed at the reactor Saphir in Würenlingen, using a triple-axis spectrometer. The measurements were carried out in the constant- Q mode of operation in the neutron energy loss configuration with the analyzer energy kept fixed at 121 cm^{-1} .

3. Theory

We interpret the magnetic susceptibility with the same spin-Hamiltonian operator as Prins et al.⁷ and Zvarykina et al.,⁸ but we include intermolecular exchange by introduction of two molecular fields.

3.1. The Isolated Molecule. The ground state of an axial molecule having spin $S = 1$ can be described by the spin-Hamiltonian operator (see e.g. ref 22)

$$\hat{H} = D[\hat{s}_z^2 - 2/3] + \mu_B \vec{H} \cdot \vec{g} \cdot \vec{s} \quad (1)$$

where D is the axial zero-field-splitting parameter and \vec{g} the axial \vec{g} tensor having elements g_{\perp} and g_{\parallel} . The splitting of the energy level in a magnetic field parallel to the axial zero field is shown in Figure 3.

For low magnetic fields ($D > \mu_B g H$) the static magnetic susceptibility along the principal axes of the molecule is given by

$$\chi_{\parallel} = \frac{2g_{\parallel}^2 \mu_B^2 N}{kT} \frac{e^{-(D/kT)}}{1 + 2e^{-(D/kT)}} \quad (2)$$

$$\chi_{\perp} = \frac{2g_{\perp}^2 \mu_B^2 N}{D} \frac{1 - e^{-(D/kT)}}{1 + 2e^{-(D/kT)}}$$

and for the isotropic powder susceptibility the following approximation is allowed:

$$\chi_{\text{iso}} = 1/3(\chi_{\parallel} + 2\chi_{\perp}) \quad (3)$$

At low temperatures ($D > kT$) these equations are reduced to

$$\chi_{\parallel} = 0$$

$$\chi_{\perp} = \frac{2g_{\perp}^2 \mu_B^2 N}{D} \quad (4)$$

$$\chi_{\text{iso}} = \frac{4}{3} \frac{g_{\perp}^2 \mu_B^2 N}{D}$$

and for the high-temperature region ($D < kT$) we obtain

$$\chi_i = \frac{2}{3} \frac{g_i^2 \mu_B^2 N}{kT} \quad i = \perp, \parallel \quad (5)$$

$$\chi_{\text{iso}} = \frac{2}{9} \frac{\mu_B^2 N}{kT} (g_{\parallel}^2 + 2g_{\perp}^2)$$

3.2. The Crystal of Nickelocene. Figure 2 shows a schematic view of the crystal structure of nickelocene. The two molecules in the unit cell each have their 5-fold axes nearly perpendicular (92.15° (101 K) and 90.83° (295 K), respectively) and lie almost in the ab plane (angle between 5-fold axis and ab plane 4.84° (101

(20) Seiler, P.; Dunitz, J. D. *Acta Crystallogr., Sect. B: Struct. Crystallogr. Cryst. Chem.* **1980**, *B36*, 2946.

(21) Seiler, P.; Dunitz, J. D. *Acta Crystallogr., Sect. B: Struct. Crystallogr. Cryst. Chem.* **1980**, *B36*, 2255.

(22) Carlin, R. L.; van Duyneveldt, A. J. *Magnetic Properties of Transition Metal Compounds*; Inorganic Chemistry Concepts 2; Springer: New York, 1977.

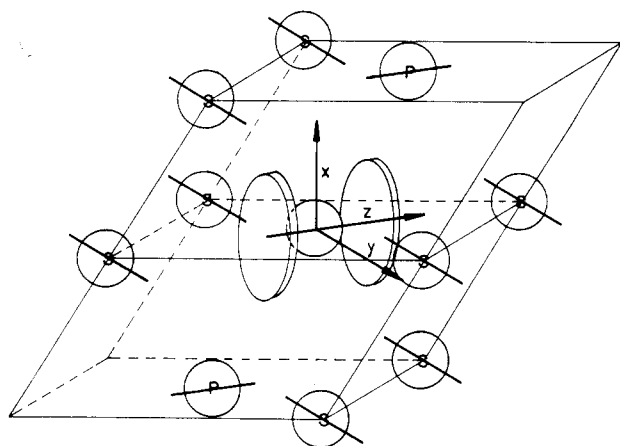


Figure 4. Molecular coordinate system for the molecular field model in nickelocene.

K) and 2.14° (295 K), respectively).²¹ Idealizing the structure with the two angles being 90° and 0° , respectively, we can deduce the following expressions for the susceptibility of a single crystal:

$$\begin{aligned} \text{in the } ab \text{ plane: } \chi_{ab} &= \frac{1}{2}(\chi_{\parallel} + \chi_{\perp}) \\ \text{perpendicular to the } ab \text{ plane: } \chi_{c^*} &= \chi_{\perp} \end{aligned} \quad (6)$$

These equations hold exactly for a crystal without any interaction between the molecules. To describe the intermolecular coupling, we define a molecular axis system as shown in Figure 4. Since there are two types of magnetically inequivalent neighboring molecules, we introduce two molecular fields for the parallel (P) and the perpendicular (S) neighbors, respectively. We then can write the magnetic susceptibility along the principal axes of a molecule in the internal fields of its neighbors as

$$\begin{aligned} \chi'_x &= \frac{\chi_{\perp}}{1 - 2\lambda_{\perp}(\Gamma_P + \Gamma_S)\chi_{\perp}} \\ \chi'_y &= \frac{\chi_{\perp}}{1 - 2(\lambda_{\perp}\Gamma_P\chi_{\perp} + \lambda_{\parallel}\Gamma_S\chi_{\parallel})} \\ \chi'_z &= \frac{\chi_{\parallel}}{1 - 2(\lambda_{\parallel}\Gamma_P\chi_{\parallel} + \lambda_{\perp}\Gamma_S\chi_{\perp})} \\ \chi'_{iso} &= (\chi'_x + \chi'_y + \chi'_z)/3 \\ \chi'_{c^*} &= \chi'_x \end{aligned} \quad (7)$$

where Γ_P and Γ_S denote the molecular field constants of the "parallel" and "perpendicular" neighbors, respectively, and λ_i is a constant $\lambda_i = (Ng_i^2\mu_B^2)^{-1}$.²² χ_i and χ'_i stand for the susceptibilities of the "isolated" and the "coupled" molecule.

Considering that χ_{\parallel} (eq 4) vanishes at low temperatures, we obtain

$$\begin{aligned} A = \frac{\chi'_{c^*}}{\chi'_{iso}} &= 3 \left(\frac{1 - 2\lambda_{\perp}\Gamma_P\chi_{\perp}}{2 - 2\lambda_{\perp}\chi_{\perp}(2\Gamma_P + \Gamma_S)} \right) \\ B = \frac{\chi'_{c^*}}{\chi'_{ab}} &= 2 \frac{1 - 2\lambda_{\perp}\Gamma_P\chi_{\perp}}{1 - 2\lambda_{\perp}(\Gamma_P + \Gamma_S)\chi_{\perp}} \end{aligned} \quad (8)$$

In the absence of any coupling $A = 3/2$ and $B = 2$, respectively. From measurements at low temperatures of $\chi'_{iso}(T)$, $\chi'_{c^*}(T)$, and $\chi_{\perp}(T)$ we can deduce the molecular field constants

$$\begin{aligned} \Gamma_P &= \frac{3\chi'_{iso}(0) - \chi'_{c^*}(0) - \chi_{\perp}(0)}{2\lambda_{\perp}(3\chi'_{iso}(0) - \chi'_{c^*}(0))\chi_{\perp}(0)} \\ \Gamma_S &= \frac{2\chi'_{c^*}(0) - 3\chi'_{iso}(0)}{2\lambda_{\perp}\chi'_{c^*}(0)(3\chi'_{iso}(0) - \chi'_{c^*}(0))} \end{aligned} \quad (9)$$

3.3. Inelastic Neutron Scattering. The magnetic moment of a neutron can interact with the magnetic moment of an electron, whereby an electron transition may be induced. The differential

cross section of a transition $|S\rangle \rightarrow |S'\rangle$ in an INS experiment is given by²³

$$\frac{d^2\sigma}{d\Omega d\omega} = \left[\frac{\gamma_e^2}{m_e c^2} \right]^2 \left[\frac{1}{2} g F(\vec{Q}) \right]^2 [\exp[-2W(\vec{Q})]] \frac{k_1}{k_0} \left[\sum_{\alpha} \left[1 - \left(\frac{Q_{\alpha}}{Q} \right)^2 \right] \right] \left[\sum_{\lambda, \lambda'} p_{\lambda} |\langle \lambda | \hat{S}^{\alpha} | \lambda' \rangle|^2 \delta(\hbar\omega + E_{\lambda} - E_{\lambda'}) \right] \quad (10)$$

where \vec{Q} is the scattering vector, \vec{k}_0 and \vec{k}_1 are the wavevectors of incoming and outgoing neutrons, respectively, $\gamma = 1.913$ (the neutron magnetic moment in units of the nuclear magneton), λ and λ' are the wave functions of the initial and final electronic levels, E_{λ} and $E_{\lambda'}$ are the energies of wave functions λ and λ' , respectively, p_{λ} is the population of the state λ , $\alpha = x, y, \text{ or } z$, m_e is the mass of the electron, $g = [J(J+1) - L(L+1) + S(S+1)]/[2J(J+1)] + 1$ (Landé factor), $F(\vec{Q}) = \langle j_0 \rangle + [(g - g_s)/g] \langle j_z \rangle$ (magnetic form factor), and $\exp[-2W(\vec{Q})]$ is the Debye-Waller factor. The remaining symbols have the usual meaning.

The great advantage of INS compared with other spectroscopic techniques lies in the possibility of unambiguously discriminating between transitions of vibrational and magnetic origin. First, with increasing modulus of the scattering vector Q the intensity of vibrational scattering increases approximately as Q^2 , whereas for magnetic excitations the intensity of scattered neutrons decreases according to the square of the magnetic form factor $F^2(\vec{Q})$. Second, the temperature dependence of neutrons scattered by phonons is governed by Bose statistics, whereas the intensity of magnetic origin follows the Boltzmann population of the initial state. Third, if a new band is observed after deuteration of the sample, this intensity unambiguously corresponds to a magnetic transition, since the incoherent proton cross section is at least one order of magnitude larger than those of any other nucleus.

4. Results

4.1. Magnetic Susceptibility. Figures 5 and 6 show some representative measurements together with theoretical curves, according to eq 2 and 7, respectively.

4.2. Inelastic Neutron Scattering. In Figure 7 several INS powder spectra of $\text{Ni}(\text{C}_5\text{D}_5)_2$ taken with different Q and temperature values, respectively, are reproduced. Clearly the band at $31.6 \pm 1.0 \text{ cm}^{-1}$ diminishes in intensity with increasing modulus of Q and temperature, respectively. In Figure 8 the intensity of this band is plotted as a function of Q .

Within experimental accuracy, no energy dispersion could be observed.

5. Discussion

Since the zero-field splitting D_0 was evaluated from the measurement of the diluted samples without knowing the concentration of guest molecules in the host, this procedure should be discussed in more detail:

Knowing that the measured force due to the paramagnetic guest molecule is constant at very low temperature, we can define a value $q(T)$, which is the ratio of the measured force at any temperature to the constant force at low temperature

$$q(T) = \frac{\Delta F'(T)}{\Delta F'(0)} = \frac{e^{-\epsilon}(g_{\parallel}^2\epsilon - 2g_{\perp}^2) + 2g_{\perp}^2}{4g_{\perp}^2e^{-\epsilon} + 2g_{\perp}^2} \quad (11)$$

$$\epsilon = D/kT$$

where $\Delta F'$ is the measured force on the Faraday balance minus the diamagnetic contribution. Because we dealt with diluted samples, the diamagnetic contribution could be estimated under the assumption that the sample consists of host molecules only. Since all samples contained less than 10% guest molecules and moreover only $q(T)$ values were used where the paramagnetic contribution to the force was dominant, this is a good approximation. In fact, the value of D evaluated by comparing the

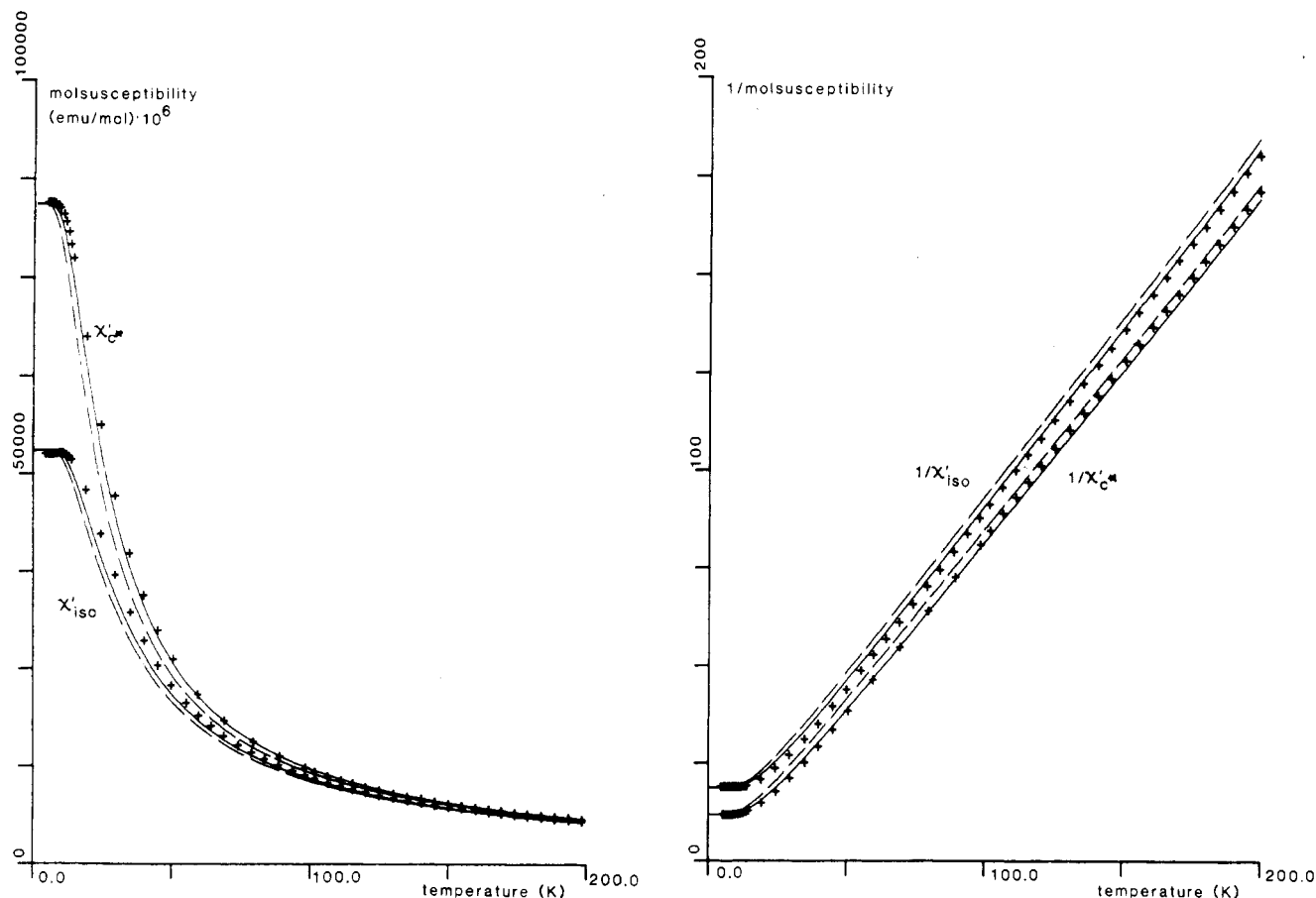


Figure 5. Magnetic susceptibility and inverse susceptibility of nickelocene at $H_0 = 9.89$ kG (temperature range = 4.4–218 K; χ'_{iso} = isotropic powder value; χ'_{c^*} = value measured on an "oriented" powder in high magnetic field (see text)); (—) calculated with parameters from Table II (eq 7); (---) calculated from spin Hamiltonian without molecular field (eq 2), with $D_{\text{eff}} = 29.2$ cm^{-1} (χ_{iso}) and $D_{\text{eff}} = 27.5$ cm^{-1} (χ_{\perp}) (D values calculated from eq 4).

Table I. Zero-Field-Splitting Parameters D_{eff} of Nickelocene Doped into Ruthenocene and Ferrocene

host	D_{eff}^a cm^{-1}	concn, ^b % of wt
ruthenocene	35.82 ± 0.22 (53)	6.00
ruthenocene	35.52 ± 0.21 (57)	4.72
ferrocene	34.70 ± 0.46 (39)	3.34
ruthenocene	34.95 ± 0.36 (43)	2.48
ruthenocene	33.76 ± 0.70 (27)	0.95

^a Mean value with statistical variation. Number of points in parentheses. ^b Evaluated from D_{eff} , g_{\perp} , and $\Delta F'(0)$; see text.

experimental $q(T)$ with the calculated value from eq 11 changed only within experimental error when the diamagnetic susceptibility of the host was altered by 10%. The zero-field splitting D_{eff} for each sample evaluated by this procedure showed a slight, continuous variation with concentration, which should not be observable for isolated molecules. The constant paramagnetic susceptibility at low temperature was calculated from eq 4 by using the values of g_{\perp} and D_{eff} . The concentration of guest molecules in each sample was then evaluated with $\Delta F'(0)$ and this calculated susceptibility. The results from several measurements are listed in Table I. The zero-field splitting $D_0 = 33.6 \pm 0.3$ cm^{-1} for the isolated nickelocene was found by extrapolation of D_{eff} for infinite dilution.

The change to larger D_{eff} values (smaller constant susceptibility at low temperatures with same g_{\perp}) with increasing concentration is probably due to an increasing antiferromagnetic intermolecular coupling in the diluted sample. Since the probability of finding a second triplet molecule in the neighborhood of the guest molecule increases with increasing concentration, we never had a perfect isolated nickelocene without any interaction in our samples. In contrast, the measurements of the undiluted samples show a ferromagnetic interaction (Γ_S and Γ_P positive, smaller D_{eff} (see

Table II. Parameters Determining the Magnetic Susceptibility of Nickelocene

$g_{\parallel} = 2.0023$ (theory ²⁷)	
$g_{\perp}^a = 2.11 \pm 0.03$	$\Gamma_P^c = 0.63$ cm^{-1}
$D_0^b = 33.6 \pm 0.3$ cm^{-1}	$\Gamma_S^c = 0.89$ cm^{-1}
$A(\text{undiluted}) = 1.59 \pm 0.03$	$A(\text{diluted: 4.72\%}) = 1.47 \pm 0.03$

^a From slope of $(\chi'_{c^*})^{-1}$ vs T at high temperature ($T \geq 150$ K), calculated by using eq 5 and neglecting effects of molecular fields at high temperature. In fact, the initial value of g_{\perp} is about 1% higher because of this assumptions. This discrepancy does not affect the evaluation of other parameters however. ^b Extrapolation for infinite dilution; for details, see text. ^c Calculated from eq 9, with g_{\perp} , D_0 , and the experimental values $\chi'_{c^*}(0)$ and $\chi'_{\text{iso}}(0)$.

Figure 5)). This discrepancy may be explained by competitive interactions:

The intermolecular coupling of a nickelocene molecule to its nearest neighbors in a first sphere in the undiluted sample is predominantly ferromagnetic, while the interaction with triplet state molecules at greater distances in the diluted sample is antiferromagnetic. In the diluted samples studied here there are almost no nearest-neighbor interactions. From EPR spectra of doublets doped into nickelocene¹¹ we know that, in the sum over pairwise interaction, giving the molecular field constants Γ_P and Γ_S for undiluted samples, antiferromagnetic as well as ferromagnetic coupling occurs, confirming this explanation. This conclusion makes it reasonable to take the zero-field-splitting parameter D_0 for an isolated molecule as the extrapolated value for infinite dilution.

The parameters for the interpretation of the magnetic susceptibility of nickelocene, both the coupled and the isolated molecule, are listed in Table II.

The disagreement between our D value and the value reported by Prins et al.⁷ is probably due to a partial orientation of the

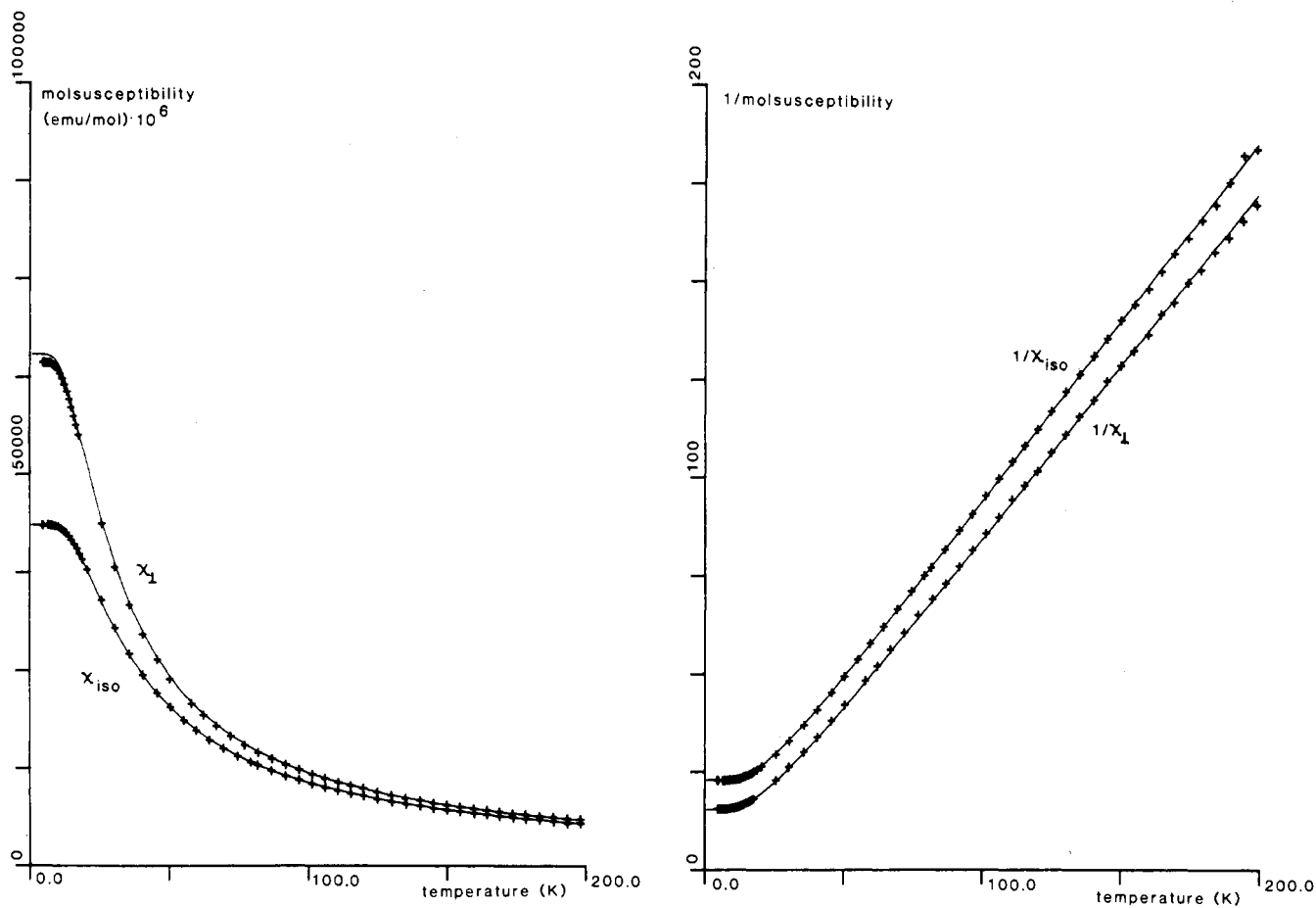


Figure 6. Magnetic susceptibility and inverse susceptibility of nickelocene in ruthenocene (4.72%) at $H_0 = 19.2$ kG (temperature range = 4.4–198 K; χ_{iso} = isotropic powder value; χ_{\perp} = value measured on an "oriented" powder in high magnetic field (see text)): (—) calculated (eq 2) with $D_{\text{eff}} = 35.52$ cm^{-1} (Table I) without molecular field.

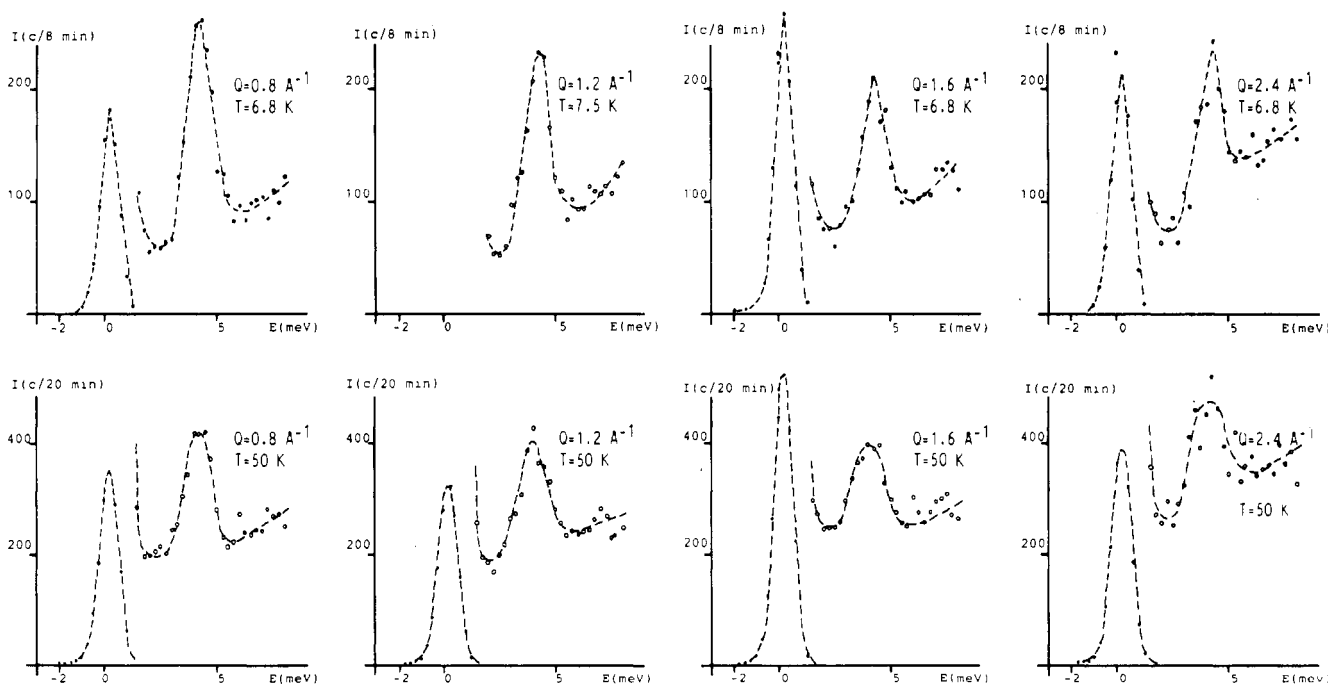


Figure 7. Inelastic neutron scattering spectra of fully deuterated nickelocene between -16 and $+65$ cm^{-1} for a series of values of Q , at 6.8 and 50 K, where Q is the modulus of the scattering vector Q . The dotted curves represent the least-squares fits to the experimental data, assuming a linear background and approximating the peaks by Gaussians. For high Q and temperature values the analysis becomes more difficult because the background of elastic scattered neutrons increases.

nickelocene crystallites. Since they used the pondero motoric method²⁴ for susceptibility measurements, it is possible that, due

to the movement of the sample during measurement, an orientation of crystallites takes place in the applied magnetic field and

(24) Rathenau, W.; Snoek, J. L. *Philips Res. Rep.* 1946, 1, 239.

(25) Hardgrove, G. L.; Templeton, D. H. *Acta Crystallogr.* 1959, 12, 28.

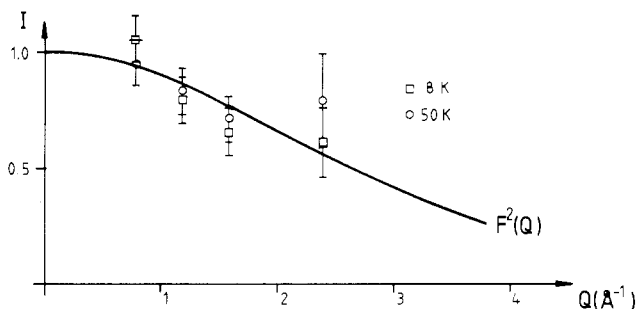


Figure 8. Q dependence of intensity of the magnetic transition at 31.6 cm^{-1} in fully deuterated nickelocene measured at 6.8 and 50 K. For the plotted function the magnetic form factor $F(Q)$ was taken from ref 26.

therefore a too large value of susceptibility is measured, leading to a smaller value of D .

The intensity of the band at $31.6 \pm 1.0 \text{ cm}^{-1}$ in the INS experiments decreases as $F^2(Q)$ with increasing Q (Figure 8). This evidence proves the magnetic nature of this transition. Furthermore, the decrease in intensity of the magnetic transition on increasing temperature in Figure 7 is in qualitative agreement with what is expected on the basis of relative Boltzmann populations of the singlet and triplet levels. Estimating the intensity of the magnetic transition at high temperature is rather difficult because of the underlying elastic scattered neutrons.

There is a slight discrepancy between the zero-field splitting D_0 found from susceptibility measurements and the energy difference ΔE measured by INS. This is probably due to the different samples, since the INS experiments were performed with undiluted nickelocene with deuteriated ligands. The observed magnetic

transition at 31.6 cm^{-1} in the INS spectra does not correspond to the zero-field splitting of an isolated molecule D_0 but will show some influence of the intermolecular coupling. One might think of the excited level of the triplet ground state in the undiluted sample as being a band of levels due to intermolecular coupling, the center of which need not be at the same energy level as in the isolated molecule.

6. Concluding Remarks

By introduction of two molecular fields describing the intermolecular interaction in undiluted nickelocene, we interpret the magnetic susceptibility of this compound, undiluted and doped into an isostructural diamagnetic host, by the *same* spin-Hamiltonian parameters. Furthermore the results of susceptibility measurements and INS investigations are in good agreement, confirming our approach. The accuracy of the zero-field-splitting parameter D_0 determined from susceptibility measurements is unique.

We have also shown the advantage of measuring the magnetic susceptibility on an oriented powder sample. Of course, one can only use this technique if the crystal structure of the compound investigated is known and the preferred orientation is almost perfect, as in our experiments. In most cases the orientation will be partial only, and a straightforward interpretation of such a measurement will be impossible. Anyway, the unwelcome effect of a spontaneous orientation of crystallites with anisotropic magnetic susceptibility should never be underestimated, and samples for isotropic powder measurements in a magnetic field have to be mechanically fixed. This may be performed as reported earlier.¹⁹

Acknowledgment. This work was supported by the Swiss National Science Foundation (Project 2.442.0.82). We thank Prof. Dr. J. H. Ammeter for helpful discussion.

Registry No. $\text{Ni}(\text{C}_5\text{H}_5)_2$, 1271-28-9; $\text{Ni}(\text{C}_5\text{D}_5)_2$, 51510-35-1.

(26) Watson, R. E.; Freeman, A. J. *Acta Crystallogr.* **1961**, *14*, 27.

(27) Prins, R.; van Voorst, J. D. W. *J. Chem. Phys.* **1968**, *49*, 4665.

Contribution from the Department of Chemistry, University of California, Irvine, California 92717

Bis(nitroxyl) Adducts of Cobalt and Nickel Hexafluoroacetylacetonates. Preparation, Structures, and Magnetic Properties of $\text{M}(\text{F}_6\text{acac})_2(\text{proxyl})_2^1$ ($\text{M} = \text{Co}^{2+}, \text{Ni}^{2+}$)

Leigh C. Porter, Michael H. Dickman, and Robert J. Doedens*

Received July 27, 1987

Bisadducts of the cyclic nitroxyl radical 2,2,5,5-tetramethylpyrrolidiny-1-oxy (proxyl) with nickel(II) and cobalt(II) hexafluoroacetylacetonates have been prepared and characterized by crystal structure analyses and magnetic susceptibility studies. The adducts are isostructural, each having a centrosymmetric molecular structure and a slightly distorted octahedral configuration about the metal ion. The O-bound nitroxyls adopt a trans configuration. Magnetic susceptibility data (6–300 K) indicate that antiferromagnetic coupling of ligand and metal free spins yields an $S = 1/2$ ground state for $\text{M} = \text{Co}^{2+}$ and an $S = 0$ ground state for $\text{M} = \text{Ni}^{2+}$. At higher temperatures, there is some population of excited states with greater spin multiplicities. Possible orbital interactions that could account for the magnetic behavior are discussed. Crystal data for $\text{Co}(\text{F}_6\text{acac})_2(\text{proxyl})_2$: monoclinic, space group $P2_1/c$, $Z = 2$, $a = 10.339$ (4) Å, $b = 14.533$ (4) Å, $c = 11.973$ (4) Å, $\beta = 111.09$ (2)°. Least-squares refinement based upon 1615 data with $F_o^2 > 3\sigma(F_o^2)$ and $2\theta \leq 50^\circ$ converged to $R = 0.056$. Crystal data for $\text{Ni}(\text{F}_6\text{acac})_2(\text{proxyl})_2$: monoclinic, space group $P2_1/c$, $Z = 2$, $a = 10.243$ (5) Å, $b = 14.564$ (5) Å, $c = 11.902$ (5) Å. Least-squares refinement based upon 1609 nonzero data with $2\theta \leq 45^\circ$ converged to $R = 0.052$.

Introduction

There has been increasing interest in compounds that contain one or more nitroxyl radicals coordinated to a transition-metal ion.²⁻²⁰ Such systems have been shown to exhibit diverse types

of magnetic behavior, including antiferromagnetic and ferromagnetic exchange of varying magnitudes, diamagnetism, and

- (1) Abbreviations for ligand names used in this paper include the following: tempo = 2,2,6,6-tetramethylpiperidiny-1-oxy; proxyl = 2,2,5,5-tetramethylpyrrolidiny-1-oxy; nitphen = 2-phenyl-4,4,5,5-tetramethylimidazoline-1-oxy-3-oxide; F_6acac = hexafluoroacetylacetonato.
- (2) Richman, R. M.; Kuechler, T. C.; Tanner, S. P.; Drago, R. S. *J. Am. Chem. Soc.* **1977**, *99*, 1055-1058.
- (3) Drago, R. S.; Kuechler, T. C.; Kroeger, M. *Inorg. Chem.* **1979**, *18*, 2337-2342.
- (4) Anderson, O. P.; Kuechler, T. C. *Inorg. Chem.* **1980**, *19*, 1417-1422.

- (5) Dickman, M. H.; Doedens, R. J. *Inorg. Chem.* **1981**, *20*, 2677-2681 and references therein.
- (6) Laugier, J.; Ramasseul, R.; Rey, P.; Espie, J. C.; Rassat, A. *Nouv. J. Chim.* **1983**, *7*, 11-14.
- (7) Grand, A.; Rey, P.; Subra, R. *Inorg. Chem.* **1983**, *22*, 391-394.
- (8) Porter, L. C.; Dickman, M. H.; Doedens, R. J. *Inorg. Chem.* **1983**, *22*, 1962-1964.
- (9) Benelli, C.; Gatteschi, D.; Zanchini, C. *Inorg. Chem.* **1984**, *23*, 798-800.
- (10) Bencini, A.; Benelli, C.; Gatteschi, D.; Zanchini, C. *J. Am. Chem. Soc.* **1984**, *106*, 5813-5818.
- (11) Beck, W. *Inorg. Chim. Acta* **1985**, *99*, L33.
- (12) Porter, L. C.; Doedens, R. J. *Inorg. Chem.* **1985**, *24*, 1006-1010.